Received: 28 May 2019 | Revised: 25 July 2019 | Accepted: 25 July 2019

DOI: 10.1111/pce.13637

ORIGINAL ARTICLE

WILEY Plant, Cell & Environment

Deficiency of very long chain alkanes biosynthesis causes humidity-sensitive male sterility via affecting pollen adhesion and hydration in rice

Bo Yu[1,2] | Lingtong Liu[1] | Tai Wang[1,2,3]

[1] Key Laboratory of Plant Molecular Physiology, Institute of Botany, Chinese Academy of Sciences, Beijing, China

[2] College of Life Science, University of Chinese Academy of Sciences, Beijing, China

[3] Innovative Academy of Seed Design, Chinese Academy of Sciences, Beijing, China

Correspondence
T. Wang, Key Laboratory of Plant Molecular Physiology, Institute of Botany, Chinese Academy of Sciences, Beijing, China.
Email: twang@ibcas.ac.cn

Funding information
Ministry of Science and Technology of the People's Republic of China, Grant/Award Number: 2013CB945101

Abstract

Pollen adhesion and hydration are the earliest events of the pollen–stigma interactions, which allow compatible pollen to fertilize egg cells, but the underlying mechanisms are still poorly understood. Rice pollen are wind dispersed, and its pollen coat contains less abundant lipids than that of insect-pollinated plants. Here, we characterized the role of *OsGL1-4*, a rice member of the Glossy family, in pollen adhesion and hydration. *OsGL1-4* is preferentially expressed in pollen and tapetal cells and is required for the synthesis of very long chain alkanes. *osgl1-4* mutant generated apparently normal pollen but displayed excessively fast dehydration at anthesis and defective adhesion and hydration under normal condition, but the defective adhesion and hydration were rescued by high humidity. Gas chromatography–mass spectrometry analysis suggested that the humidity-sensitive male sterility of *osgl1-4* was probably due to a significant reduction in C25 and C27 alkanes. These results indicate that very long chain alkanes are components of rice pollen coat and control male fertility via affecting pollen adhesion and hydration in response to environmental humidity. Moreover, we proposed that a critical point of water content in mature pollen is required for the initiation of pollen adhesion.

KEYWORDS

humidity-sensitive male sterility, pollen adhesion, pollen hydration, rice, very long chain alkane

1 | INTRODUCTION

Pollination in angiosperms involves multiple interactions between pollen and stigma including adhesion, hydration, germination, and tube invasion (Dresselhaus & Franklin-Tong, 2013; Edlund, Swanson, & Preuss, 2004; Swanson, Edlund, & Preuss, 2004). This process is highly selective in the species with dry stigmas, whose surfaces are covered with waxy cuticles and lack sticky secretions of wet stigmas (Edlund et al., 2004); thus, pollen tubes need to overcome surface barriers of the stigma to allow pollen adhesion and tube invasion (Doucet, Lee, & Goring, 2016). The compatibility is established in a short time window when compatible pollen grains adhere to the papillae and then access stigmatic water for hydration, which allow subsequent pollen germination and tube invasion (Doucet et al., 2016). Therefore, pollen adhesion is a prerequisite for pollen hydration, and it is crucial for reproductive selection and successful reproduction (Chapman & Goring, 2010; Doucet et al., 2016; Edlund et al., 2004; Firon, Nepi, & Pacini, 2012).

Studies of *Brassicaceae* including *Arabidopsis* and *Brassica* plants have revealed cytological characteristics of pollen adhesion and identified several pollen coat–derived factors implicated in pollen adhesion and hydration. Pollen coat (also called pollenkitt or tryphine) is a pollen extracellular matrix, which fills the space and cavities of the highly sculpted exine (Rejón et al., 2016). Pollen grains of *Arabidopsis* and *Brassica* are completely surrounded by abundant pollen coat, main components of which are lipids, followed by diverse proteins

(Mayfield, Fiebig, Johnstone, & Preuss, 2001; Murphy, 2006), and can survive in vitro for long time. Previous study showed that uncharacterized lipophilic components of pollen exine were involved in initial adhesion step (Zinkl, Zwiebel, Grier, & Preuss, 1999). Following the exine-mediated initial adhesive interaction, proteins and lipids from pollen coat are considered to be implicated in the subsequent stronger adhesive interactions (Chapman & Goring, 2010). At this stage, pollen coat is supposed to mobilize onto the stigmatic papilla to form a "pollen foot" between the pollen and stigmatic surface, and the pollen foot allows water and self-compatible signal exchange between the cells (Elleman & Dickinson, 1986; Elleman, Franklin-Tong, & Dickinson, 1992). Poor adhesion was observed for pollen lacking coat from *Arabidopsis* mutants and coat-removed pollen from *Brassica oleracea* (Chapman & Goring, 2010; Edlund et al., 2004). In *Brassica*, pollen coat protein (PCP) *SLR1-BP* and *PCP-A1* are involved in pollen adhesion via binding S-locus glycoprotein and S-locus related-1, respectively (Doughty et al., 1998; Takayama et al., 2000). Mutation in *Arabidopsis PCP-B* led to defective pollen adhesion and hydration (Wang et al., 2017).

The pollen foot is proposed to act as a capillary system for rapid flow of water, nutrients, and other small molecules from the papilla into pollen grains, which leads to pollen hydration and germination (Chapman & Goring, 2010; Edlund et al., 2004). Finally, the pollen tube passes through the foot into the stigmatic papilla, tethering the empty pollen grain to the stigma via the tube (Edlund et al., 2004). Pollen adhesion regulators derived from the pollen coat are less known, whereas progresses have been made in identifying pollen coat–derived molecules required for pollen hydration in *Arabidopsis*. Studies of *Arabidopsis* have reported that mutation in oleosin-domain–containing glycine-rich protein (GRP) 17, extracellular lipase 4 (EXL4), and KINβγ subunit of SnRK1 complex led to defective pollen hydration (Aarts, Keijzer, Stiekema, & Pereira, 1995; Fiebig et al., 2000; Gao et al., 2016; Mayfield & Preuss, 2000; Updegraff, Zhao, & Preuss, 2009). Very long chain fatty acids (VLCFAs) and their derivatives such as aldehydes, alcohols, alkanes, ketones, and wax esters are constituents of epicuticular waxes. Accumulation of epicuticular waxes in *Arabidopsis* is regulated by more than 20 *ECERIFERUM* (*CER*) loci (Aarts et al., 1995). *CER1* and *CER6* are involved in pollen hydration. *CER1* is mainly expressed in stems, flowers, and siliques and predicted to encode an aldehyde decarboxylase catalysing the conversion of aldehyde to alkane, a key step in wax biosynthesis (Aarts et al., 1995). *CER1* and *CER3* may form a complex to accomplish the synthesis of VLC alkanes, and they are main components to composite the enzymatic activity (Bernard et al., 2012). *CER6* is mainly expressed in stems, leaves, and flowers and required for the production of VLCFAs (Fiebig et al., 2000). *cer1* mutant displayed wax-deficient stem and reduction of lipid droplets in pollen coat, whereas *cer6* mutant showed the absence of all classes of long-chain lipids in stem cuticle and pollen coat, thus had no pollen coat. Pollen grains of the two mutants were defective in hydration and displayed male sterility in low-humidity environment, but the male sterility could be rescued in high-humidity condition (Aarts et al., 1995; Bourdenx et al., 2011; Fiebig et al., 2000; Hannoufa, Mcnevin, & Lemieu, 1993; Preuss, Lemieux, Yen, & Davis, 1993). Although these studies have made much progress in elucidating the mechanisms of pollen adhesion and hydration in *Brassicaceae* plants, there is less mechanistic understanding of the process in wind-pollinated plants. It is known that there is great mechanistic diversity in diverse species, which is important to reproduction isolation of species (Escobar-Restrepo et al., 2007).

Rice (*Oryza sativa*) is one of the most important crops in the world, and the model experimental material of monocots, and also is a representative of *Gramineae* plants. In contrast to *Brassicaceae* such as *Arabidopsis* and *Brassica*, rice pollen grains have much less coat with unidentified lipids (Dai et al., 2006; Mayfield et al., 2001; Murphy, 2006); the pollen can survive in vitro only in minutes after anthesis under natural conditions (Dai et al., 2006). It is known that water content of pollen grains during dispersal is associated with pollen viability. *Gramineae* pollen grains contain higher water content (>30%) than *Brassicaceae* pollen grains but lose water easily. The former is considered as desiccation sensitive and lose viability quickly, and the latter as desiccation tolerant and decrease viability gradually at low relative humidity (RH). It has been proposed that desiccation-sensitive pollen grains lack the mechanisms to keep water content within certain limits (Firon et al., 2012). Studying the mechanisms of water-holding capacity of rice pollen and subsequent pollen adhesion and hydration is important both for our understanding of pollen–stigma interaction in planta and for developing molecular designer approaches to monitor crop male fertility for crop production, but our knowledge is limited. In rice, Glossy (GL) family is involved in the accumulation of epicuticular waxes. Among 11 rice GL sequences, *OsGL1-5/Wax-Deficient Anther1* (*WDA1*) has been reported for the involvement in anther development. This gene was highly expressed in panicles. Its mutation led to defective epidermal layer and tapetum of anthers and significant deficits in wax constituents. Thus, the mutant was devoid of mature pollen grains in anthers due to the degeneration of meiocytes (Jung et al., 2006). This suggested functional diversity of long-chain lipids in reproduction of monocots and dicots. A recent study demonstrated that rice mutant in *OsOSC12/OsPTS1* encoding a bicyclic triterpene synthase was defective in pollen hydration in low-humidity condition and showed humidity-sensitive male sterility. This enzyme converts 2,3-oxidosqualene to a diverse set of functional steroids and triterpenoids, which are supposed to be components of rice pollen coat (Xue et al., 2018).

Here, we dissected the mechanisms of pollen adhesion and hydration using loss-of-function mutants of *OsGL1-4*, a member of the GL family in rice. The mutant had no alternation in growth and development and generated viable pollen grains, which normally germinated and gave rise to pollen tubes in vitro. We imaged morphological changes of pollen in response to environmental humidity and observed interaction of pollen and stigmatic papilla using live-cell imaging. The mutant pollen showed unusually fast water loss as compared with wild-type (WT) pollen and had humidity-dependent pollen adhesion and hydration, thus displaying humidity-sensitive male sterility. Furthermore, mutation in *OsGL1-4* significantly

decreased the production of the C25 and C27 alkanes and led to aberrant pollen coat. These data reveal promising strategies to monitor male fertility of rice by improving the resistance of pollen to environmental stress and by generating novel humidity-sensitive male sterile lines.

2 | MATERIALS AND METHODS

2.1 | Plant materials

Rice plants (*O. sativa* ssp. *japonica* cv. *Nipponbare*) were grown in a growth room under a 12-hr photoperiod with normal humidity (30–60% RH) or high humidity (>80% RH) at 25–35°C. The *OsGL1-4* mutants were generated by CRISPR-cas9 system.

2.2 | Phylogenetic analysis

The full-length amino acid sequence of *OsGL1-4* protein was used as the query to search for its closest relatives in published databases, National Center for Biotechnology Information and The Arabidopsis Information Resource. Multiple sequences were aligned with the ClustalW tool, and a phylogenetic tree was constructed by use of MEGA programme.

2.3 | Quantitative RT-PCR analysis

Total RNA was isolated from various tissues by using the RNeasy Plant Mini Kit (QIAGEN). The rice tissues used included roots, leaves, pistils, and anthers. The developmental stages of anthers were categorized according to the spikelet length (Zhang, Luo, & Zhu, 2011). A 0.5 μg of total RNA was used for reverse transcription by using Super Script III reverse transcriptase (Invitrogen). The primers used were qRTC2F1(TCCCATATCACAGTTCCCCC) and qRTC2R1(TCTTGGAAG CCAATTCTCGC).

2.4 | In situ hybridization

Anthers were fixed in FAA (50% v/v ethanol, 5% v/v acetic acid, and 3.7% v/v formaldehyde) for 16 hr at 4°C. After dehydration through ethanol series and through a xylene–ethanol series, the anther was embedded in Paraplast (Sigma), sectioned at 9-μm slices by using an RM2235 rotary microtome (Leica), and mounted onto Poly-Prep slides (Matsunami). These slices were hybridized to either a sense or an antisense *OsGL1-4* probe, and signals were detected as described previously (Xue et al., 2018).

2.5 | Subcellular localization

The coding sequence of *OsGL1-4* was cloned into a modified pCAMBIA1302 vector to produce a Ubi::OsGL1-4-GFP construct. The construct was cotransformed with an endoplasmic reticulum (ER) marker fusion (mCherry-CD3-959) into rice protoplasts. Transformed protoplasts were incubated in the dark at 28°C for 16 hr and then observed under a confocal microscope (Olympus FV1000 MPE). Images were captured at 488 nm for GFP excitation and 543 nm for RFP excitation.

2.6 | Pollen viability examination

For Alexander staining, anthers were immersed in Alexander's solution for 2 days at room temperature. The stained anthers were stripped off to release pollen grains for microscopy observation. For 4′,6-diamidino-2-phenylindole (DAPI) staining, pollen grains were fixed in Carnoy's solution (30% chloroform, 10% acetic acid, and 57% ethanol) for 2 hr at room temperature, stained in DAPI solution for 20 min in the dark, and imaged under a microscope.

2.7 | Pollen dehydration and germination assay

To measure the rate of pollen dehydration, pollen grains from a freshly dehisced anthers were released onto a dry glass slide, and their morphological changes were observed under a microscope. The percentage of shrunken pollen grains in the observed total pollen grains was described as pollen dehydration rate.

For pollen germination in vitro, pollen grains were shed onto a solid germination medium, incubated, and observed as described previously (Liu et al., 2016). In vivo pollen tube growth in pistils was observed by using naturally pollinated pistils at 5 hr after anthesis. The pollinated pistils were fixed in Carnoy's solution for 2 hr, washed five times with water, softened in 1-mol/L NaOH for 55°C for 30 min, and stained in aniline blue solution in the dark at 4°C overnight. Images were obtained with a ZEISS microscope (Axio Imager A1) under ultraviolet light.

2.8 | Pollen adhesion and hydration examination

To observe pollen adhesion and hydration, pistils before anthesis were cut and put on agar (1%) and then pollinated manually. Humidity condition in the environment was regulated by use of the humidifier. Behaviours of the pollen grain in stigma were tracked under a microscope.

Pollen adhesion was further observed in vivo. Number of pollen grains in self-pollinated pistils at 2 hr after pollination was counted directly or after aniline blue staining with a ZEISS microscope.

2.9 | Scanning electron microscopy

Pollen grains and pollinated pistils were fixed in FAA for 24 hr at 4°C, dehydrated through a graded ethanol, passed through an ethanol–isoamyl acetate series, and finally dried with CO_2 critical point. The dried samples were mounted on stubs, coated with gold, and examined using a Hitachi S-4800 device (Hitachi).

2.10 | Transmission electron microscopy

Anthers and pollen grains were processed as described previously (Xue et al., 2018). The samples were infiltrated in Spurr's resin and London Resin White, respectively. Sections were observed by ZEISS microscope and JEM-1230 device (JEOL), respectively.

2.11 | Mass spectrometry of VLCFAs

Anthers and pollen grains waxes were analysed as described previously (Jung et al., 2006). Ten milligrams of freeze-dried anthers or pollen grains was submersed in 1-ml chloroform and then crushed with an ultrasonic crusher for about 30 min. One microgram of tetracosane was used as an internal standard. The solvent was evaporated under a nitrogen stream. The sample was added with 30-μl pyridine and 30-μl bis-(*N*,*N*-trimethylsilyl)-tri-fluoroacetamide (BSTFA) and incubated at 70°C for 50 min. The wax composition was determined with gas chromatography–mass spectrometry analysis.

3 | RESULTS

3.1 | *OsGL1-4* is preferentially expressed in anthers

Our transcriptome analysis revealed that *OsGL1-4*, a GL family member of rice, was expressed in pollen with higher levels in tricellular pollen and mature pollen than in microspores and bicellular pollen (Wei et al., 2010). Further analysis of transcripts in anther and pollen showed that *OsGL1-4* transcripts were highly accumulated in developing anthers and were at relatively low level in leaves but rarely detected in pistils, roots, and stems (Figure 1a). In anthers, this gene showed decreased expression as anther developed. RNA in situ hybridization revealed strong signals in tapetal cells and tricellular pollen (Figure 1b). Together, these results demonstrated that *OsGL1-4* was expressed preferentially in anthers and the transcript was confined to tapetal cells and late stages of pollen development.

Phylogenetic analysis showed that the 11 rice GL protein sequences were organized into three groups. *OsGL1-4* was in a clade with *OsGL1-7* and *OsGL1-5*, which were closed to *OsGL1-6* and *Arabidopsis CER1* and *CER1*-like (Figure 1c). *OsGL1-5* and *CER1* have been identified for wax biosynthesis (Aarts et al., 1995; Jung et al., 2006). These sequences shared His-rich motifs HX3HH, HXHHH, and HX2HH (Figure S1). The His residues in the three conserved His-rich motifs are supposed to provide the ligands for a presumed catalytic Fe centre, which are essential for the catalytic activity for sterol desaturases (Taton, Husselstein, Benveniste, & Rahier, 2000). All the three His-rich motifs in *CER1* are essential for VLC alkane synthesis (Bernard et al., 2012). Thus, these results suggest that *OsGL1-4* is likely involved in VLCFA metabolism, especially in VLC alkane biosynthesis in rice.

3.2 | *OsGL1-4* is required for male fertility

In order to study the function of *OsGL1-4*, we obtained two independent loss-of-function mutant lines through CRISPR-Cas9 system, *osgl1-4* and *osgl1-4a*, which harbour frameshift mutations at respective target site (Figure 2a). Mutants were backcrossed to WT plants to eliminate possible interference from tissue culture. *osgl1-4* and *osgl1-4a* had no significant difference with WT plants in growth and development (Figure S2a). However, self-pollinated *osgl1-4* and *osgl1-4a* only had 4.1% and 6.3% seed setting rate, in contrast to 90.1% for WT (Figure 2b,c). This indicated that mutation in *OsGL1-4* led to defective fertility. Thus, we characterized the function of *OsGL1-4* using the allelic mutant *osgl1-4* in detail. We examined whether the sterility was from defective male or/both female transmission via the reciprocal crosses between *osgl1-4* and WT plants under RH of 30–60%. When mutant pistils were pollinated with WT pollen grains, all the F_1 plants showed WT phenotype, and the F_2 progeny displayed a segregation of 3:1 (χ^2 = 2.01, p > .05), indicating that *osgl1-4* is a recessive single-gene mutation. Although WT pistils pollinated with *osgl1-4*, pollen grains rarely produced seeds (Figure S3a,b). This indicated the defective male transmission.

This mutant had normal panicles and floral organs, and flowering was normal (Figures 3a,b and S2b). Pollen grains of mutant and WT plants showed no obvious difference in Alexander staining (Figure 3c–f), and both contained one loosely stained vegetative nucleus and two condensed sperm nuclei (Figure S2c). Next, we examined in vitro pollen germination. Under normal conditions, 81.08% of *osgl1-4* pollen grains germinated, which was comparable with the germination rate of WT pollen grains (Figure 3i). The germinated pollen grains both from mutant and WT plants can gave rise to normal pollen tubes (Figure 3 g,h). Together, these data indicated that mutation in *OsGL1-4* did not affect pollen viability, germination, and tube growth.

3.3 | *osgl1-4* shows defective pollen adhesion and hydration

Our results clearly indicated that *osgl1-4* plants can generate viable pollen grains, which normally germinate and gave rise to pollen tubes in the germination medium. Thus, we further observed the effect of RH on pollen fertility of *osgl1-4*. We carried out the reciprocal crosses of *osgl1-4* plants with WT plants under RH >80% and showed that WT pistils pollinated with *osgl1-4* pollen grains gave rise to normal seed setting rate, which was comparable with that of *osgl1-4* pistils pollinated with WT pollen grains (Figure S3c,d). This is in contrast to the results of reciprocal crosses of *osgl1-4* and WT plants under 30–60% RH (Figure S3a,b). These results suggested that *osgl1-4* pollen sterility is humidity sensitive.

Furthermore, we examined water retention ability of pollen grains under 30–60% RH by shedding mature pollen grains at anthesis onto a dry glass slide and observing time-lapse morphological

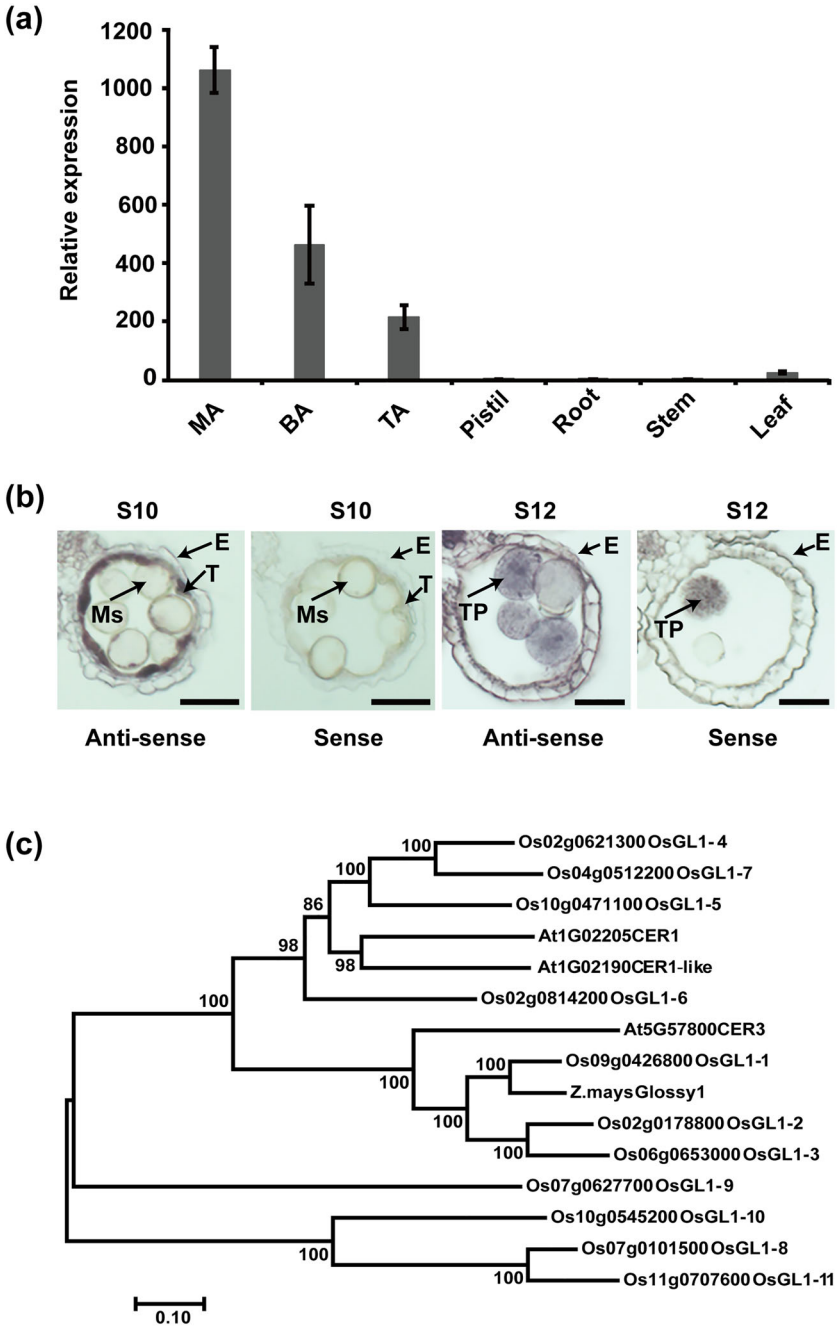

FIGURE 1 Expression patterns and phylogenic feature of *OsGL1-4*. (a) qRT-PCR of *OsGL1-4* transcripts in anther at microspore stage (MA), bicellular pollen stage (BA), tricellular pollen stage (TA), pistil, root, stem, and leaf. (b) In situ hybridization of *OsGL1-4* transcripts in anthers at S10 (uninucleate pollen) and S12 (tricellular pollen) stages with the sense probe used as the negative control. E, epidermis; Ms, microspore; TP, tricellular pollen; T, tapetum. Scale bars, 50 μm. (c) A neighbour-joining phylogenic tree indicating phylogenic relation of *OsGL1-4* with related sequences from *Oryza sativa* (Os), *Arabidopsis thaliana* (At), and *Zea mays*. The length of the branches refers to the amino acid variation rates

changes. Most WT pollen grains showed no morphological changes within 1 min, whereas all *osgl1-4* pollen grains shrank within 30 s. Specifically, WT pollen underwent only a mild dehydration before 1 min and dehydrated thereafter, whereas *osgl1-4* pollen grains dehydrated immediately as they were placed onto the glass slide and become fully dehydrated within 30 s (Figure 2d,e and Movies S1 and S2). We also observed the adhesion and hydration on stigma under 30–60% RH. As being pollinated on the papilla, the WT pollen grain fast formed pollen foot appearance on the stigma cell, which represented stronger adhesive interactions (Chapman & Goring, 2010), hydrated (round appearance), and then showed germination and tube invasion (Figure 4a and Movie S3), whereas the mutant pollen grain did not demonstrate the pollen foot appearance and thus did not hydrate (shrunken appearance). However, once RH was increased, the shrunken mutant pollen grain established pollen foot on the papillae, hydrated, and displayed phenotype of germination and tube invasion (Figure 4b and Movie S4). This was consistent with the seed setting rate of mutants under two different RHs: 4.1% and 6.3%, under 30–60% RH versus 82.9% and 82.2% under >80% RH (Figure 4c,d).

To clarify the effect of *OsGL1-4* on pollen adhesion to stigma, we further collected self-pollinated pistils of mutant and WT plants at 2 hr after flowering pollination and counted pollen amount on pistils directly and after aniline blue staining. The average number of pollen grains on each untreated and treated self-pollinated WT pistil was 95.9 and 60.46, respectively, whereas the respective amount on

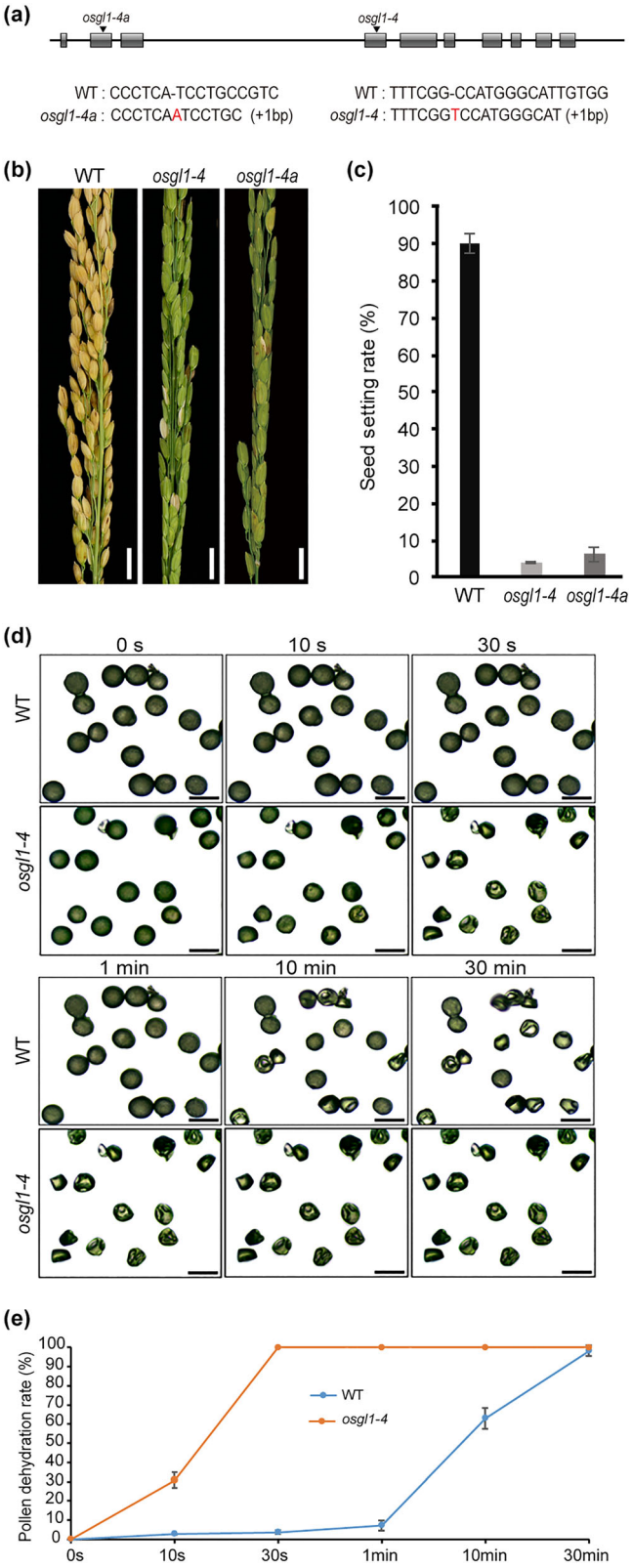

FIGURE 2 *osgl1-4* pollen grains show aberrant dehydration. (a) *osgl1-4* mutation sites edited by CRISPR-Cas9 system. Boxes and lines indicate the *OsGL1-4* exons and introns, respectively. The insertion nucleotides are marked in red. (b) Panicles of wild-type (WT) and *osgl1-4* and *osgl1-4a* plants at seed maturity stage. (c) Seed setting rate of WT and *osgl1-4* and *osgl1-4a* plants. The data are presented as mean ± *SD*, *n* = 15. (d) Time-lapse images of WT and *osgl1-4* pollen grains in vitro under 30–60% relative humidity. (e) Dehydration rate of WT and *osgl1-4* pollen grains. The data are presented in the form of mean ± *SD*. Scale bars: 1 cm in (b) and 50 μm in (d)

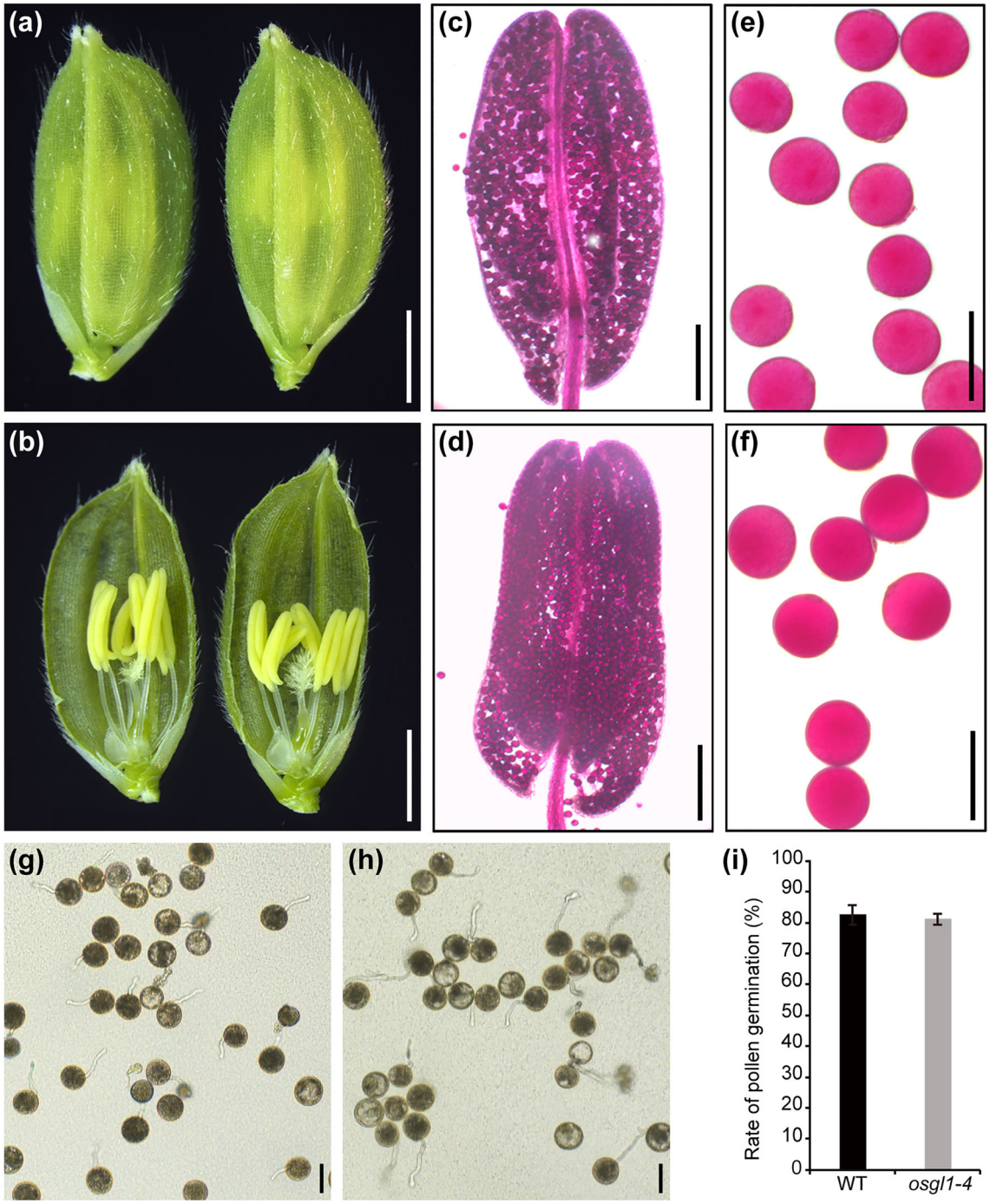

FIGURE 3 *osgl1-4* pollen are normally stained and produce pollen tubes in vitro. (a) Wild type (WT; left) and *osgl1-4* (right) spikelet. (b) Palea-removed spikelet of WT (left) and *osgl1-4* (right) to indicate stamens and the pistil. (c,d) Alexander staining of WT (c) and *osgl1-4* (d) anthers. (e, f) Alexander staining of WT (e) and *osgl1-4* (f) pollen grains. (g,h) In vitro pollen germination of WT (g) and *osgl1-4* (h). (i) Pollen germination rate. The data are presented as mean ± *SE*. Scale bars: 2 mm in (a,b), 200 μm in (c,d), and 50 μm in (e–h)

untreated and treated self-pollinated *osgl1-4* pistils was 64.5 and 2.93 (Figure 5a–g). Observation of pistils at 5 hr after flowering pollination showed that WT ovules were targeted by pollen tubes with the empty pollen grains tethered to the stigma, whereas the mutant did not show ovules targeted by pollen tubes and the empty pollen grains in the stigma. Collectively, these results indicated the defective pollen adhesion and hydration in mutant pollen.

3.4 | OSGL1-4 is required for VLC alkane synthesis

Scanning electron microscopy showed that the anther surfaces and epicuticular wax crystals appeared to be unaffected in *osgl1-4* mutant (Figure 6a–d). The WT pollen grain was round, whereas the *osgl1-4* pollen appeared shrunken (Figure 6e,f). Transverse section analysis of anther development showed that there was no significant

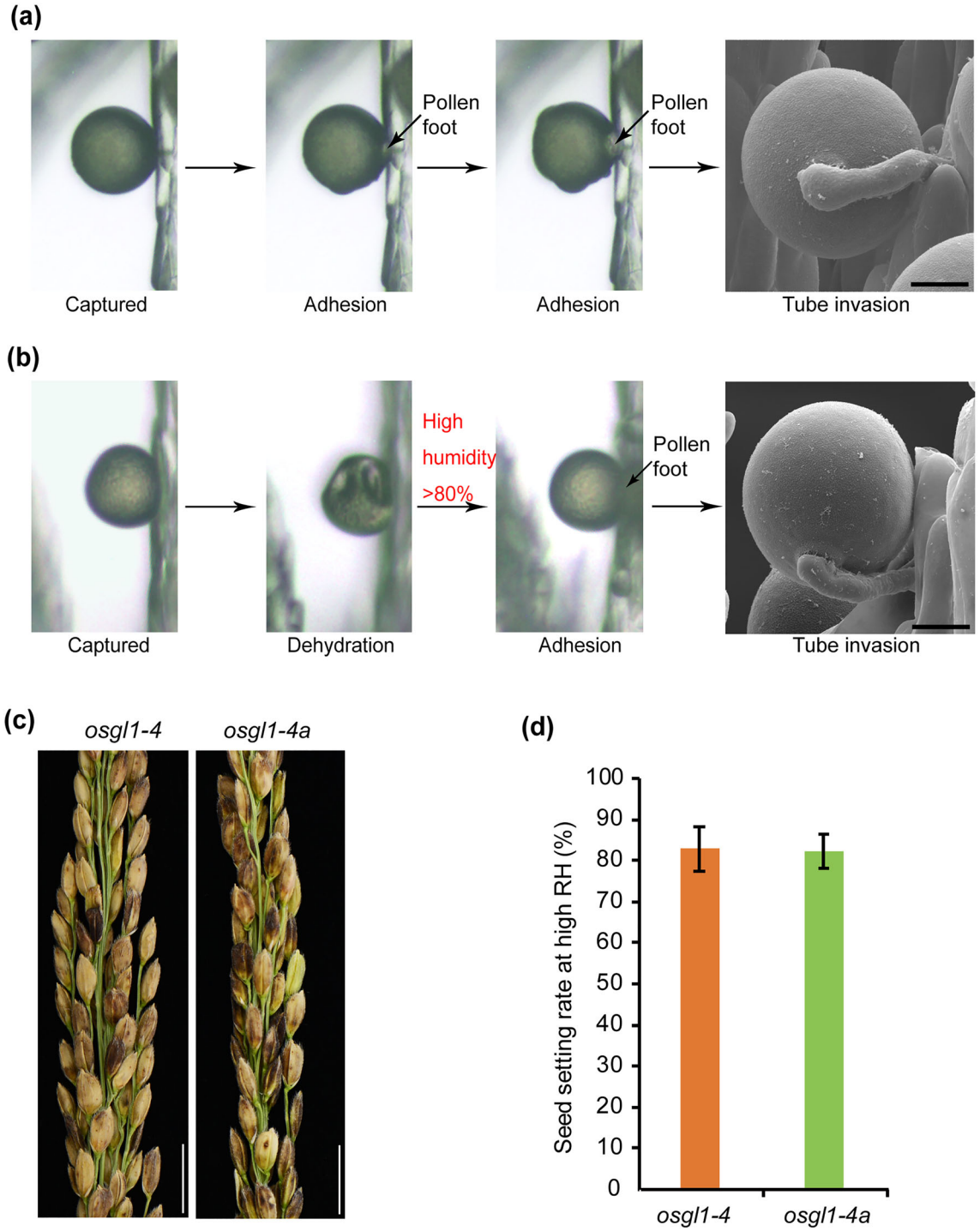

FIGURE 4 *osgl1-4* pollen grains display humidity-dependent adhesion and hydration. (a,b) Time-lapse images of (a) wild-type (WT) and (b) *osgl1-4* pollen grains interact with stigma papillae. WT pollen pollinated onto papilla experiences adhesion and hydration and then germination and tube invasion into stigma. However, only in high humidity, *osgl1-4* pollen acts similar to WT pollen (see also Movies S3 and S4). The tube invasion image is obtained by use of scanning electron microscopy. (c,d) Panicles of *osgl1-4* and *osgl1-4a* plants treated with high humidity at mature stage (c) and their seed setting rate (d). The data are presented as mean ± *SD*. Scale bars: 10 μm in (a,b) and 1 cm in (c)

difference in *osgl1-4* compared with WT (Figure S4). Transmission electron microscopy revealed that the *osgl1-4* pollen had complete exine and apparently normal development of tapetum but was deficient in pollen coat components, as compared with the WT pollen grain (Figures 6g,h and S5).

OsGL1-4 is an integral membrane protein with five predicted transmembrane domains. We determined the subcellular localization of *OsGL1-4* by expressing OsGL1-4-GFP fusion in rice protoplasts. OsGL1-4-GFP was colocalized with the ER marker mCherry-CD3-959, thus indicating that *OsGL1-4* was located in the ER (Figure 7a).

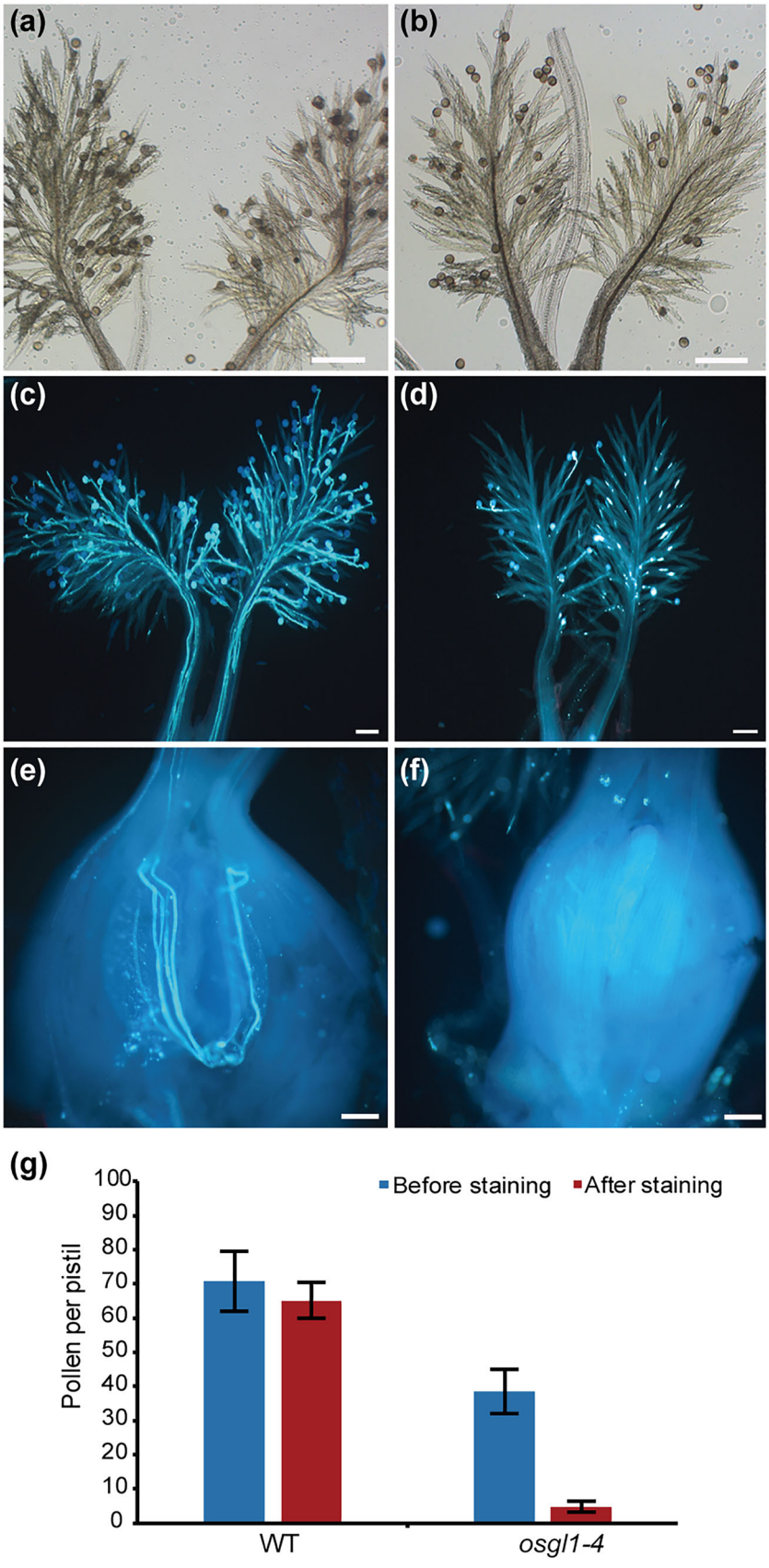

FIGURE 5 The absence of pollen adhesion and tube invasion in *osgl1-4* pistils. (a,b) Bright-field images of pistils at 2 hr after pollination from wild type (a) and *osgl1-4* (b) before aniline blue staining. (c–f) Pollen tube growth in pistils at 5 hr after pollination of wild type (c,e) and *osgl1-4* (d,f). (g) Pollen number per pistil before and after aniline blue staining. Results are presented as mean ± *SE*. Scale bars: 200 μm in (a,b) and100 μm in (c–f)

This is consistent with the fact that most of the wax synthesis enzymes in *Arabidopsis* and rice are in the ER (Bernard et al., 2012; Wang et al., 2017; Zhou et al., 2015).

Because bioinformatics analysis suggests that *OsGL1-4* is likely involved in VLCFA metabolism, especially in alkane biosynthesis, we characterized VLCFA and its derivatives from *osgl1-4*, *osgl1-4a*,

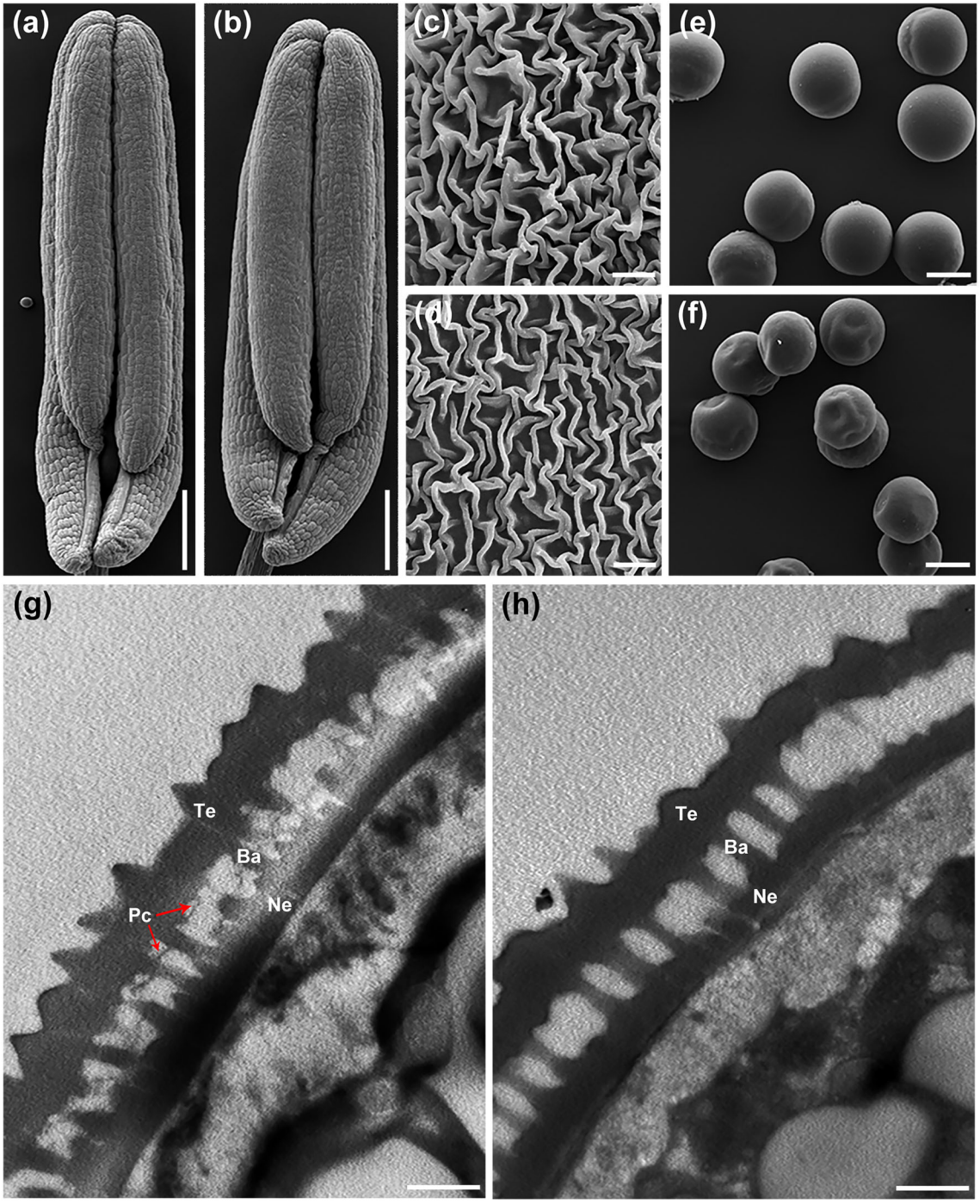

FIGURE 6 *osgl1-4* pollen has deficient pollen coat. (a,b) Scanning electron microscopy images of (a) wild type (WT) and (b) *osgl1-4* anthers. (c,d) Close-up of the anther epidermal surface of (c) WT and (d) *osgl1-4*. (e,f) Scanning electron microscopy images of (e) WT and (f) *osgl1-4* pollen grains. (g,h) Transmission electron microscopy images of (g) WT and (h) *osgl1-4* pollen wall. Ba, bacula; Ne, nexine; Pc, pollen coat; Te, tectum. Scale bars: 200 μm in (a,b), 2 μm in (c,d), 20 μm in (e,f), and 0.5 μm in (g,h)

and WT anthers. Total wax loads of *osgl1-4* and *osgl1-4a* anthers were reduced by 31.5% and 62.5% as compared with WT anthers (Table 1). The mutation in *OsGL1-4* had different effects on wax constituents. Alkanes contents in *osgl1-4* and *osgl1-4a* anthers were reduced by 64.4% and 69.2%: The changed alkanes involved C23–C29 alkanes. C23 alkanes were decreased by 31.3% and 39.8%, C25 alkanes by 93.3% and 87.7%, C27 alkanes by 87.8% and 89.5%, and C29 alkanes by 33.4% and 45.6%. The changed VLCFAs involved C18, C20, C24, and C26 fatty acids, and changed alcohols mainly involved C26 alcohol (Figure 7b; Table S1).

Total wax loads of *osgl1-4* pollen grains were reduced by 64.6% as compared with WT pollen grains (Table 2). Alkanes contents in *osgl1-4* pollen grains were reduced by 81.2%: The changed alkanes

involved C23–C33 alkanes. C23 alkanes were decreased by 60.7%, C25 alkanes by 85.3%, C27 alkanes by 89.9%, C29 alkanes by 79.9%, C31 alkanes by 38%, and C33 alkanes by 57.9% (Figure 7c; Table S2). This indicated that *OsGL1-4* is required for VLC alkane synthesis. Collectively, these results demonstrated that decreased VLC alkanes led to deficient pollen coat.

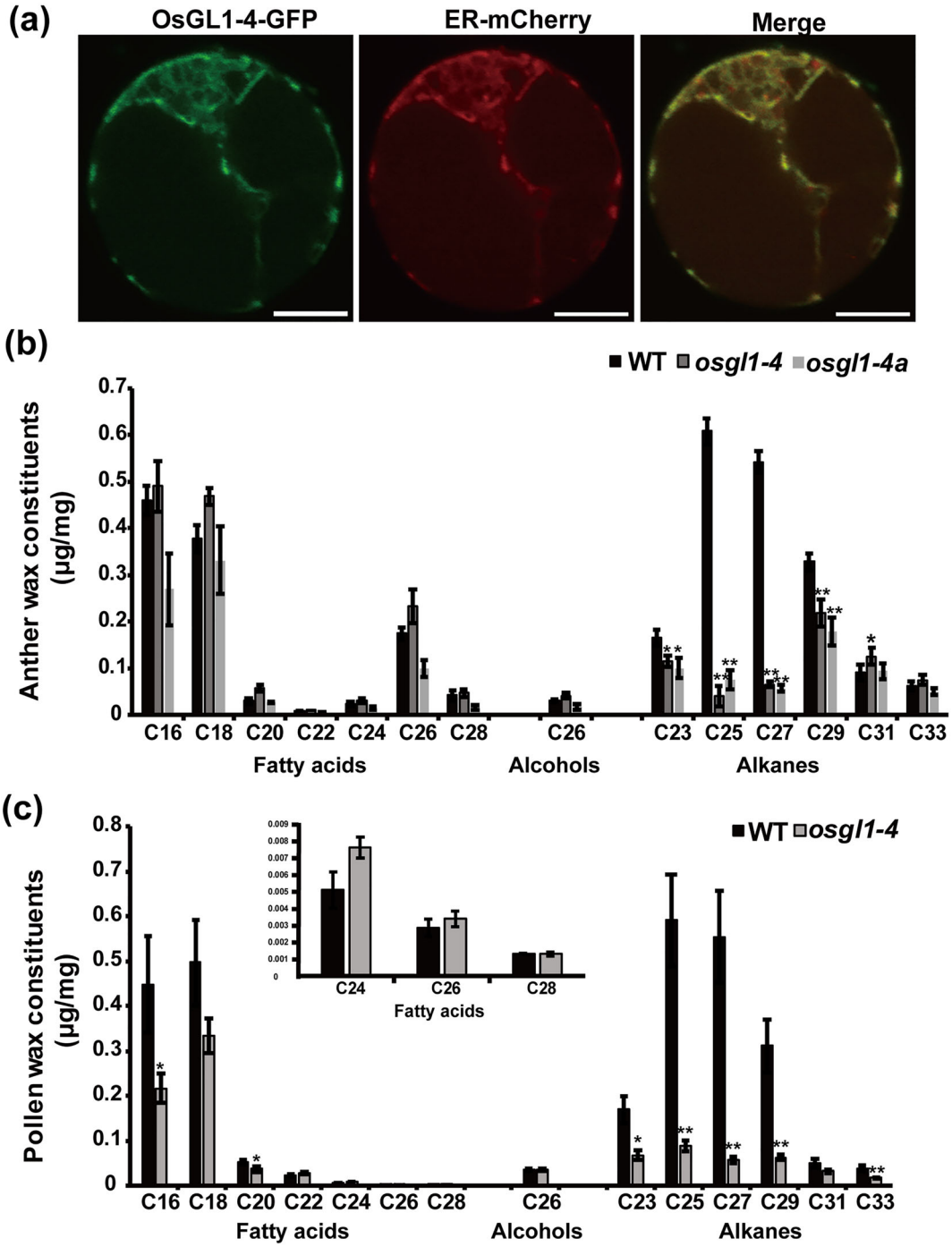

FIGURE 7 Subcellular localization of *OsGL1-4* and wax components of anthers and pollen grains. (a) The green and red signals obtained with confocal microscopy indicated fusion proteins OsGL1-4-GFP and ER-mCherry (ER marker protein), respectively. The overlap of GFP and mCherry fluorescent signals is indicated in merged images. Scale bar: 10 μm. (b) Content of each wax component of anthers of WT and *osgl1-4* and *osgl1-4a* plants. Results are presented as mean ± *SD* of three biological replicates. $^{**}p < .01$. (c) Content of each wax component of pollen grains of WT and *osgl1-4* plants. Results are presented as mean ± *SD* of three biological replicates. $^{**}p < .01$

TABLE 1 Wax compositions of anthers from wild-type and *osgl1-4* and *osgl1-4a* plants

Wax contents	WT (μg/mg) (Mean ± *SD*)	*osgl1-4* (μg/mg) (Mean ± *SD*)	*osgl1-4a* (μg/mg) (Mean ± *SD*)
Fatty acid	1.117 ± 0.031	1.339 ± 0.054	0.767 ± 0.177
Alcohol	0.030 ± 0.002	0.041 ± 0.006	0.016 ± 0.006
Alkane	1.800 ± 0.078	0.640 ± 0.081	0.555 ± 0.099
Total	2.948 ± 0.158	2.020 ± 0.198	1.106 ± 0.196

Note. Data are mean ± *SD* of three biological replicates.

Abbreviation: WT, wild type.

TABLE 2 Wax compositions of pollen grains from wild-type and *osgl1-4* plants

Wax contents	WT (μg/mg) (Mean ± *SD*)	*osgl1-4* (μg/mg) (Mean ± *SD*)
Fatty acid	1.029 ± 0.208	0.626 ± 0.079
Alcohol	0.035 ± 0.006	0.035 ± 0.002
Alkane	1.714 ± 0.309	0.322 ± 0.038
Total	2.778 ± 0.523	0.984 ± 0.119

Note. Data are mean ± *SD* of three biological replicates.

4 | DISCUSSION

4.1 | VLC alkanes are pollen coat components and essential for pollen adhesion and hydration in rice

We have showed that *OsGL1-4* is an ER-localized aldehyde decarboxylase involved in VLC alkane biosynthesis. *osgl1-4* mutants grew and developed normally and generated two sperm cells containing viable pollen, which can germinate and give rise to pollen tubes in vitro. However, this mutation led to significantly decreased contents of VLC alkanes, especially C25 and C27 alkanes in anthers and pollen grains with defective pollen coat, clearly indicating that the alkanes are components of rice pollen coat. Thus, we first provide molecular and biochemical evidences that VLC alkanes are in pollen coat of rice, a representative of wind-pollinated plants. Tapetum is believed to play a major role in pollen coat formation in *Brassica*, but little information is available in monocots including rice (Rejón et al., 2016). High expression levels of *OsGL1-4* both in developing pollen and tapetum suggest that pollen itself may also contribute to VLC lipids of pollen coat.

OsGL1-4 was in a clade with *OsGL1-7* and *OsGL1-5*/*WDA1*, which were closed to *OsGL1-6* and *Arabidopsis CER1* in the phylogenetic tree. *OsGL1-4*, *OsGL1-5*, and *CER1* have been identified to be involved in VLC alkane biosynthesis (this study; Bernard et al., 2012; Jung et al., 2006), but their biological function appeared diversified. *Arabidopsis CER1* was required for pollen hydration with preferential expression in stems, flowers, and siliques (Aarts et al., 1995), and *OsGL1-5* was required for pollen development via affecting the epidermal layer and tapetum of anther wall with preferential expression in epidermis of floral organs (Jung et al., 2006). Because pollen adhesion and hydration on the stigma occur in a short time window, we observed *osgl1-4* pollen behaviour on stigma by live-cell imaging. Clearly, WT pollen formed pollen foot on the stigma, a cytological character of stronger adhesive interactions (Chapman & Goring, 2010), whereas *osgl1-4* pollen did not form pollen foot under normal humidity condition; thus, the pollen appeared shrinking. This was consistent with the absence of pollen adhesion and pollen tube growth in the mutant pistils. With increasing environmental humidity, the mutant pollen can form pollen foot on the stigma and then appeared round. Consistently, the high-humidity–treating mutant had a seed setting rate comparable with WT plants. So the VLC alkanes are essential for pollen adhesion and hydration in rice, and their deficiency leads to humidity-sensitive male sterility. This appeared to be different from roles of VLC alkanes in *Arabidopsis* in pollen–stigma interactions, which were reported for the involvement in pollen hydration but not in pollen adhesion (Aarts et al., 1995; Bourdenx et al., 2011; Fiebig et al., 2000). So our study provides novel knowledge about mechanisms of pollen adhesion. Interestingly, genome-wide transcriptomics analysis of pollen showed expression of other three GL family genes: *OsGL1-1*, *OsGL1-10*, and *OsGL1-11*, in rice pollen (Wei et al., 2010), which were phylogenetically organized into different branches with *OsGL1-4*. Collectively, these results suggest that wax constituents may have other functions in pollen beyond the role in pollen adhesion and hydration.

4.2 | Regulation of VLC alkane biosynthesis in pollen represents a mechanism to keep pollen water content with certain limits for the initiation of pollen adhesion

Rice pollen is desiccation sensitive and loses viability within minutes during dispersal. It is considered that the type of pollen lacks mechanisms for retaining water content and the mechanisms involve water channels, osmoregulation under water stress, and accumulation of specific proteins such as LEA proteins and dehydrins (Firon et al., 2012). We revealed that most of WT rice grains lost water and became shrunk in 10 min, whereas *osgl1-4* pollen grains all lost water and became shrunk in 10 s as being released from anthers in normal RH. The immediate loss of pollen water led to defective pollen adhesion and male sterility. However, the defective pollen adhesion and male sterility were completely rescued by high RH. These results indicate that VLC alkanes in pollen coat confer the ability of pollen grains to retain critical levels of water content at a certain time. The critical level of water content is essential for initiation of pollen adhesion. Deficiency in VLC alkanes led to rapid water loss of pollen, then defective adhesion, and final male sterility. Together with the fact that rice pollen grains have much less coat, our results explained why rice pollen grains only survive for a short time after being released from anthers.

4.3 | Molecular designer–based modifying of pollen coat represents a valuable approach to generate new types of environment-sensitive male sterile crops

osgl1-4 mutants were almost completely sterile under normal RH but had more than 80% seed setting rate under high RH. Similarly, loss

of function of genes for VLC lipid metabolism in *Arabidopsis* also displayed humidity-sensitive male sterility (Aarts et al., 1995; Bourdenx et al., 2011; Fiebig et al., 2000). Together, these data reveal two promising strategies to monitor male fertility of rice, possible other cereal crops. First, increasing contents of VLC lipids in pollen coat by overexpressing the lipid biosynthesis–related genes may be feasible to improve adaption of pollen grains to stress and promote crop yield under stress. Second, new types of humidity-sensitive male sterile lines are generated by editing genes involved in VLC lipid biosynthesis. Male sterile lines are crucial for production of hybrids, which are used for increasing grain yield by taking advantage of the heterosis. The photoperiod/thermo-sensitive male sterile lines that involve long noncoding RNA or small RNA-mediated mechanism (Ding et al., 2012; Fan et al., 2016) can be used in hybrid rice, but temperature fluctuation caused by global climate changes often leads to a male sterility–fertility transition, which affects hybrid production. Recent study showed that deficiency of rice pollen coat components steroids and triterpenoids led to humidity-sensitive male sterility in rice (Xue et al., 2018). Collectively, these results indicate that molecular designer–based modifying of pollen coat will be valuable approaches to generate new types of environment-sensitive male sterile materials for crop production.

ACKNOWLEDGEMENTS

We thank Lu Wang for the support with mass spectrometry and Fengqin Dong for assistance with electron microscope. This research was funded by the Ministry of Science and Technology of the People's Republic of China (Grant 2013CB945101).

AUTHOR CONTRIBUTIONS

Tai Wang planned and designed the research and wrote the manuscript. Bo Yu was involved with all aspects of the research with Lingtong Liu contributing to pollen adhesion observation.

ORCID

Lingtong Liu https://orcid.org/0000-0002-1779-7330

REFERENCES

Aarts, M. G., Keijzer, C. J., Stiekema, W. J., & Pereira, A. (1995). Molecular characterization of the *CER1* gene of Arabidopsis involved in epicuticular wax biosynthesis and pollen fertility. *The Plant Cell*, *7*(12), 2115–2127.

Bernard, A., Domergue, F., Pascal, S., Jetter, R., Renne, C., Faure, J. D., … Joubès, J. (2012). Reconstitution of plant alkane biosynthesis in yeast demonstrates that Arabidopsis ECERIFERUM1 and ECERIFERUM3 are core components of a very-long-chain alkane synthesis complex. *The Plant Cell*, *24*(7), 3106–3118. https://doi.org/10.1105/tpc.112.099796

Bourdenx, B., Bernard, A., Domergue, F., Pascal, S., Léger, A., Roby, D., … Joubès, J. (2011). Overexpression of Arabidopsis ECERIFERUM1 promotes wax very-long-chain alkane biosynthesis and influences plant response to biotic and abiotic stresses. *Plant Physiology*, *156*(1), 29–45. https://doi.org/10.1104/pp.111.172320

Chapman, L. A., & Goring, D. R. (2010). Pollen–pistil interactions regulating successful fertilization in the *Brassicaceae*. *Journal of Experimental Botany*, *61*(7), 1987–1999. https://doi.org/10.1093/jxb/erq021

Dai, S. J., Li, L., Chen, T. T., Chong, K., Xue, Y. B., & Wang, T. (2006). Proteomic analyses of *Oryza sativa* mature pollen reveal novel proteins associated with pollen germination and tube growth. *Proteomics*, *6*(8), 2504–2529. https://doi.org/10.1002/pmic.200401351

Ding, J. H., Lu, Q., Ouyang, Y. D., Mao, H. L., Zhang, P. B., Yao, J. L., … Zhang, Q. F. (2012). A long noncoding RNA regulates photoperiod-sensitive male sterility, an essential component of hybrid rice. *Proceedings of the National Academy of Sciences of the United States of America*, *109*(7), 2654–2659. https://doi.org/10.1073/pnas.1121374109

Doucet, J., Lee, H. K., & Goring, D. R. (2016). Pollen acceptance or rejection: A tale of two pathways. *Trends in Plant Science*, *21*(12), 1058–1067. https://doi.org/10.1016/j.tplants.2016.09.004

Doughty, J., Dixon, S., Hiscock, S. J., Willis, A. C., Parkin, I. A., & Dickinson, H. G. (1998). *PCP-A1*, a defensin-like Brassica pollen coat protein that binds the S locus glycoprotein, is the product of gametophytic gene expression. *The Plant Cell*, *10*(8), 1333–1347. https://doi.org/10.1105/tpc.10.8.1333

Dresselhaus, T., & Franklin-Tong, N. (2013). Male–female crosstalk during pollen germination, tube growth and guidance, and double fertilization. *Molecular Plant*, *6*(4), 1018–1036. https://doi.org/10.1093/mp/sst061

Edlund, A. F., Swanson, R., & Preuss, D. (2004). Pollen and stigma structure and function: The role of diversity in pollination. *The Plant Cell*, *16*(Suppl), S84–S97. https://doi.org/10.1105/tpc.015800

Elleman, C. J., & Dickinson, H. G. (1986). Pollen–stigma interactions in Brassica. *IV. Structural reorganization in the pollen grains during hydration. Journal of Cell Science*, *80*, 141–157.

Elleman, C. J., Franklin-Tong, V., & Dickinson, H. G. (1992). Pollination in species with dry stigmas: The nature of the early stigmatic response and the pathway taken by pollen tubes. *New Phytologist*, *121*(3), 413–424. https://doi.org/10.1111/j.1469-8137.1992.tb02941.x

Escobar-Restrepo, J. M., Huck, N., Kessler, S., Gagliardini, V., Gheyselinck, J., Yang, W. C., & Grossniklaus, U. (2007). The FERONIA receptor-like kinase mediates male–female interactions during pollen tube reception. *Science*, *317*(5838), 656–660. https://doi.org/10.1126/science.1143562

Fan, Y. R., Yang, J. Y., Mathioni, S. M., Yu, J. S., Shen, J. Q., Yang, X. F., … Zhang, Q. F. (2016). PMS1T, producing phased small-interfering RNAs, regulates photoperiod-sensitive male sterility in rice. *Proceedings of the National Academy of Sciences of the United States of America*, *113*(52), 15144–15149. https://doi.org/10.1073/pnas.1619159114

Fiebig, A., Mayfield, J. A., Miley, N. L., Chau, S., Fischer, R. L., & Preuss, D. (2000). Alterations in *CER6*, a gene identical to *CUT1*, differentially affect long-chain lipid content on the surface of pollen and stems. *The Plant Cell*, *12*(10), 2001–2008. https://doi.org/10.1105/tpc.12.10.2001

Firon, N., Nepi, M., & Pacini, E. (2012). Water status and associated processes mark critical stages in pollen development and functioning. *Annals of Botany*, *109*(7), 1201–1214. https://doi.org/10.1093/aob/mcs070

Gao, X. Q., Liu, C. Z., Li, D. D., Zhao, T. T., Li, F., Jia, X. N., … Zhang, X. S. (2016). The Arabidopsis KINβγ subunit of the SnRK1 complex regulates pollen hydration on the stigma by mediating the level of reactive oxygen species in pollen. *PLoS Genetics*, *12*(7), e1006228. https://doi.org/10.1371/journal.pgen.1006228

Hannoufa, A., Mcnevin, J., & Lemieu, B. (1993). Epicuticular waxes of *eceriferum* mutants of *Arabidopsis thaliana*. *Phytochemistry*, *33*(4), 851–855. https://doi.org/10.1016/0031-9422(93)85289-4

Jung, K. H., Han, M. J., Lee, D. Y., Lee, Y. S., Schreiber, L., Franke, R., & An, G. (2006). Wax-deficient anther1 is involved in cuticle and wax production in rice anther walls and is required for pollen development. *The Plant Cell*, *18*(11), 3015–3032. https://doi.org/10.1105/tpc.106.042044

Liu, L. T., Zheng, C. H., Kuang, B. J., Wei, L. Q., Yan, L. F., & Wang, T. (2016). Receptor-like kinase RUPO interacts with potassium transporters to regulate pollen tube growth and integrity in rice. *PLoS Genetics*, *12*(7), e1006085. https://doi.org/10.1371/journal.pgen.1006085

Mayfield, J. A., Fiebig, A., Johnstone, S. E., & Preuss, D. (2001). Gene families from the *Arabidopsis thaliana* pollen coat proteome. *Science*, *292*(5526), 2482–2485. https://doi.org/10.1126/science.1060972

Mayfield, J. A., & Preuss, D. (2000). Rapid initiation of Arabidopsis pollination requires the oleosin-domain protein *GRP17*. *Nature Cell Biology*, *2*(2), 128–130. https://doi.org/10.1038/35000084

Murphy, D. J. (2006). The extracellular pollen coat in members of the *Brassicaceae*: Composition, biosynthesis, and functions in pollination. *Protoplasma*, *228*(1-3), 31–39. https://doi.org/10.1007/s00709-006-0163-5

Preuss, D., Lemieux, B., Yen, G., & Davis, R. W. (1993). A conditional sterilemutation eliminates surface components from Arabidopsis pollen and disrupts cell signaling during fertilization. *Genes & Development*, *7*(6), 974–985. https://doi.org/10.1101/gad.7.6.974

Rejón, J. D., Delalande, F., Schaeffer-Reiss, C., Alché, J. D., Rodríguez-García, M. I., Van Dorsselaer, A., & Castro, A. J. (2016). The pollen coat proteome: At the cutting edge of plant reproduction. *Proteomes*, *4*(1). https://doi.org/10.3390/proteomes4010005

Swanson, R., Edlund, A. F., & Preuss, D. (2004). Species specificity in pollen–pistil interactions. *Annual Review of Genetics*, *38*, 793–818. https://doi.org/10.1146/annurev.genet.38.072902.092356

Takayama, S., Shiba, H., Iwano, M., Asano, K., Hara, M., Che, F. S., … Isogai, A. (2000). Isolation and characterization of pollen coat proteins of *Brassica campestris* that interact with S locus-related glycoprotein 1 involved in pollen–stigma adhesion. *Proceedings of the National Academy of Sciences of the United States of America*, *97*(7), 3765–3770. https://doi.org/10.1073/pnas.040580797

Taton, M., Husselstein, T., Benveniste, P., & Rahier, A. (2000). Role of highly conserved residues in the reaction catalyzed by recombinant Delta7-sterol-C5(6)-desaturase studied by site-directed mutagenesis. *Biochemistry*, *39*(4), 701–711. https://doi.org/10.1021/bi991467t

Updegraff, E. P., Zhao, F., & Preuss, D. (2009). The extracellular lipase EXL4 is required for efficient hydration of Arabidopsis pollen. *Sexual Plant Reproduction*, *22*(3), 197–204. https://doi.org/10.1007/s00497-009-0104-5

Wang, L., Clarke, L. A., Eason, R. J., Parker, C. C., Qi, B., Scott, R. J., & Doughty, J. (2017). PCP-B class pollen coat proteins are key regulators of the hydration checkpoint in *Arabidopsis thaliana* pollen–stigma interactions. *New Phytologist*, *213*(2), 764–777. https://doi.org/10.1111/nph.14162

Wang, X. C., Guan, Y. Y., Zhang, D., Dong, X. B., Tian, L. H., & Qu, L. Q. (2017). A β-ketoacyl-CoA synthase is involved in rice leaf cuticular wax synthesis and requires a CER2-LIKE protein as a cofactor. *Plant Physiology*, *173*(2), 944–955. https://doi.org/10.1104/pp.16.01527

Wei, L. Q., Xu, W. Y., Deng, Z. Y., Su, Z., Xue, Y. B., & Wang, T. (2010). Genome-scale analysis and comparison of gene expression profiles in developing and germinated pollen in *Oryza sativa*. *BMC Genomics*, *11*(1), 338. https://doi.org/10.1186/1471-2164-11-338

Xue, Z. Y., Xu, X., Zhou, Y., Wang, X. N., Zhang, Y. C., Liu, D., … Qi, X. Q. (2018). Deficiency of a triterpene pathway results in humidity-sensitive genic male sterility in rice. *Nature Communications*, *9*(1), 604. https://doi.org/10.1038/s41467-018-03048-8

Zhang, D. B., Luo, X., & Zhu, L. (2011). Cytological analysis and genetic control of rice anther development. *Journal of Genetics and Genomics*, *38*(9), 379–390. https://doi.org/10.1016/j.jgg.2011.08.001

Zhou, X. Y., Li, L. Z., Xiang, J. H., Gao, G. F., Xu, F. X., Liu, A. L., … Wan, X. Y. (2015). *OsGL1-3* is involved in cuticular wax biosynthesis and tolerance to water deficit in rice. *PLoS ONE*, *10*(1), e116676. https://doi.org/10.1371/journal.pone.0116676

Zinkl, G. M., Zwiebel, B. I., Grier, D. G., & Preuss, D. (1999). Pollen–stigma adhesion in Arabidopsis: A species-specific interaction mediated by lipophilic molecules in the pollen exine. *Development*, *126*(23), 5431–5440.

SUPPORTING INFORMATION

Additional supporting information may be found online in the Supporting Information section at the end of the article.

Table S1 Wax compositions of anthers from wild-type, *osgl1-4* and *osgl1-4a* plants. Data are presented as mean ± SD of three biological replicates.

Table S2 Wax compositions of pollen grains from wild-type and *osgl1-4*. Data are presented as mean ± SD of three biological replicates.

Figure S1 Multiple alignments of amino acid sequences of OsGL1-4, OsGL1-5, OsGL1-6, CER1 and CER1-like. The conserved His-rich motifs are underlined.

Figure S2 Phenotypes of WT, *osgl1-4* and *osgl1-4a* plants. (a) Plant morphology of WT and *osgl1-4*, *osgl1-4a*. (b) Panicles of WT and *oagl1-4*, *osgl1-4a* plants. (c) DAPI staining of WT and *osgl1-4* pollen grains. Scale bars, 10 cm in (a), 1 cm in (b), 50 μm in (c).

Figure S3 The reciprocal crosses between *osgl1-4* and WT plants under natural condition and high humidity. (a, b) Under natural condition, *osgl1-4* pistils were pollinated with WT pollen grains (a), while WT pistils were pollinated with *osgl1-4* pollen grains (b). (c, d) Under high humidity, *osgl1-4* pistils were pollinated with WT pollen grains (c), while WT pistils were pollinated with *osgl1-4* pollen grains. Scale bars, 1 cm.

Figure S4 Cross section comparison of the anther development in WT and *osgl1-4*. The images are presented from cross-sections through single locules. WT sections are shown in (a to g) and *osgl1-4* (h to n) from stage 6 to stage 11. (a) and (h), Stage 6. (b) and (i), Stage 7. (c) and (j), Stage 8a. (d) and (k), Stage 8b. (e) and (l), Stage 9. (f) and (m), Stage 10. (g) and (n), Stage 11. BP, bicellular pollen; E, Epidermis; En, Endothecium; Ms, microspore; T, tapetum. Scale bars, 20 μm.

Figure S5 TEM analysis of pollen exine and tapetal cells in WT and *osgl1-4* from stage 8a to stage 11. (a) to (e) Cross sections of the WT pollen exine at stage 8a (a), stage 8b (b), early stage 9 (c), stage 10 (d), stage 11 (e). (f) to (j) Cross sections of the *osgl1-4* pollen exine at stage 8a (f), stage 8b (g), early stage 9 (h), stage 10 (i), stage 11 (j). (k) to (o) Cross sections of the WT tapetum at stage 8a (k), stage 8b (l), early stage 9 (m), stage 10 (n), stage 11 (o). (p) to (t) Cross sections of the *osgl1-4* tapetum at stage 8a (p), stage 8b (q), early stage 9 (r), stage 10 (s), stage 11 (t). Ba, bacula; Dy, dyad cell; Lb, lipid body; Ms,

microspore; Ne, nexine; P, plastid; PE, primexine; Te, tectum; U, ubisch body. Scale bars, 0.5 μm.

Movie S1 Live-cell imaging showing the dehydration of WT pollen grains from freshly dehisced anthers on a dry glass slide.

Movie S2 Live-cell imaging showing the dehydration of *osgl1-4* pollen grains from freshly dehisced anthers on a dry glass slide.

Movie S3 Live-cell imaging showing interaction of WT pollen grain and stigma papillae.

Movie S4 Live-cell imaging showing interaction of *osgl1-4* pollen grain and stigma papillae. Short interruption indicating an action to increase humidity.

How to cite this article: Yu B, Liu L, Wang T. Deficiency of very long chain alkanes biosynthesis causes humidity-sensitive male sterility via affecting pollen adhesion and hydration in rice. *Plant Cell Environ*. 2019;42:3340–3354. https://doi.org/10.1111/pce.13637